



Fluorinated Covalent Organic Frameworks: A Novel Pathway to Enhance Hydrogen Sorption and Control Isothermic Heats of Adsorption

HyMARC Seed Project Final Report

Justin Johnson

National Renewable Energy Laboratory

**NREL is a national laboratory of the U.S. Department of Energy
Office of Energy Efficiency & Renewable Energy
Operated by the Alliance for Sustainable Energy, LLC**

This report is available at no cost from the National Renewable Energy Laboratory (NREL) at www.nrel.gov/publications.

Contract No. DE-AC36-08GO28308

Technical Report
NREL/TP-5900-76603
December 2020



Fluorinated Covalent Organic Frameworks: A Novel Pathway to Enhance Hydrogen Sorption and Control Isothermic Heats of Adsorption

HyMARC Seed Project Final Report

Justin Johnson

National Renewable Energy Laboratory

Suggested Citation

Johnson, Justin. 2020. *Fluorinated Covalent Organic Frameworks: A Novel Pathway to Enhance Hydrogen Sorption and Control Isothermic Heats of Adsorption; HyMARC Seed Project Final Report*. Golden, CO: National Renewable Energy Laboratory. NREL/TP-5900-76603 <https://www.nrel.gov/docs/fy21osti/76603.pdf>.

**NREL is a national laboratory of the U.S. Department of Energy
Office of Energy Efficiency & Renewable Energy
Operated by the Alliance for Sustainable Energy, LLC**

This report is available at no cost from the National Renewable Energy Laboratory (NREL) at www.nrel.gov/publications.

Contract No. DE-AC36-08GO28308

Technical Report
NREL/TP-5900-76603
December 2020

National Renewable Energy Laboratory
15013 Denver West Parkway
Golden, CO 80401
303-275-3000 • www.nrel.gov

NOTICE

This work was authored by the National Renewable Energy Laboratory, operated by Alliance for Sustainable Energy, LLC, for the U.S. Department of Energy (DOE) under Contract No. DE-AC36-08GO28308. This material is based upon work supported by the Hydrogen Materials – Advanced Research Consortium (HyMARC), established as part of the Energy Materials Network under the U.S. Department of Energy, Office of Energy Efficiency and Renewable Energy, Fuel Cell Technologies Office. This report was prepared as an account of work sponsored by an agency of the United States Government. Neither the United States Government nor any agency thereof, nor any of their employees, makes any warranty, express or implied, or assumes any legal liability or responsibility for the accuracy, completeness, or usefulness of any information, apparatus, product, or process disclosed, or represents that its use would not infringe privately owned rights. Reference herein to any specific commercial product, process, or service by trade name, trademark, manufacturer, or otherwise does not necessarily constitute or imply its endorsement, recommendation, or favoring by the United States Government or any agency thereof. The views and opinions of authors expressed herein do not necessarily state or reflect those of the United States Government or any agency thereof.

This report is available at no cost from the National Renewable Energy Laboratory (NREL) at www.nrel.gov/publications.

U.S. Department of Energy (DOE) reports produced after 1991 and a growing number of pre-1991 documents are available free via www.OSTI.gov.

Cover Photos by Dennis Schroeder: (clockwise, left to right) NREL 51934, NREL 45897, NREL 42160, NREL 45891, NREL 48097, NREL 46526.

NREL prints on paper that contains recycled content.

Full budget period includes tasks:

Task 1 Fluorinated COF synthesis

- 1.1: Synthesize COF series: COF-0, COF-OH, F-COF
- 1.2: Synthesize modified linker series 1: dialdehyde linkers with N-N functionality
- 1.3: Synthesize modified linker series 2: dialdehyde linkers with OH-N functionality
- 1.4: Produce COFs from modified linker series 1 and 2: F-COF-mod1 and F-COF-mod2
- 1.5: intercalate metals into F-COF-mod1 and F-COF-mod2

Task 2 Structural Characterization of the Effect of Fluorination

- 2.1: Characterize COF series with XRD, AFM, SEM
- 2.2: Characterize COF series with NMR, FTIR/Raman
- 2.3: Characterize COF series with XPS, low-temperature FTIR

Task 3 Testing and Metrics

- 3.1: Measure BET surface area of first COF series
- 3.2: Determine isotherms and adsorption enthalpy of first COF series
- 3.3: Characterize F-COF-mod 1 series with chelated metals

Project Title: HyMARC Seed Project: Fluorinated Covalent Organic Frameworks: A Novel Pathway to Enhance Hydrogen Sorption and Control Isosteric Heats of Adsorption

Project Period: October 1, 2017 to November 30, 2018 (Note: no-cost extension was used to continue work through approximately January 15, 2019)

Date of Report: April 15, 2019

HyMARC Seed Project: Fluorinated Covalent Organic Frameworks: A Novel Pathway to Enhance Hydrogen Sorption and Control Isosteric Heats of Adsorption

Project Manager/Prin. Invest.: Justin Johnson, 303-384-6190, Justin.johnson@nrel.gov

Other Key Researchers: NREL: Wade Braunecker, Katie Hurst

Sub-Contractors Funded through Budget Period Task(s):
Alan Sellinger, Colorado School of Mines

Other collaborations:
HyMARC, HySCORE

DOE Technology Development Manager: Jesse Adams

DOE Hydrogen Storage Team Leader: Ned Stetson

Project Objective:

Our objectives are to: (i) synthesize and characterize a series of partially fluorinated covalent organic frameworks (COFs) that are intended to exhibit improved long-range ordering and assist in tuning H₂ binding enthalpy; (ii) substitute metal-chelating moieties in the framework structure to enhance H₂ binding enthalpy and demonstrate a pathway to values between 10-15 kJ/mol; (iii) tune adsorption isotherms using a target mixture of binding sites, assisted by theoretical predictions. By the end of the full project period we propose to synthesize and characterize functionalized COF materials that have necessary properties for achieving the 2020 Hydrogen Storage goals set forth by DOE, including volumetric capacities of greater than 30 g H₂/L (total system), which would require isosteric heats of hydrogen absorption >15 kJ/mol. For the initial funding period we will demonstrate that the first generation of fluorinated COFs, described below, will achieve at least 4% excess gravimetric capacity and at least 40 g H₂/L total volumetric capacity at 77K and 100 bar. In addition, the isosteric heat of adsorption will reach ≥ 10 kJ/mol for a non-metallated COF or ≥ 12 kJ/mol for a COF with intercalated metals.

Background:

Organic framework materials, as a unique sub-class of carbon-based sorbents, have gained increasing attention for promising attributes toward gas storage. Calculations of the hydrogen capacity of optimized frameworks show potential to achieve greater than 60 g/L storage of hydrogen, placing metal-organic frameworks (MOFs) and COFs near the top of the class of porous materials. However, at the ensemble level, poor stacking creates a quasi-amorphous material with low structural integrity and low effective surface area. The chemical versatility of COFs allows for additional methods for producing long-range order that specifically target the inter-layer interactions in COFs but that leave key pore-accessible linker sites open. These modifications (either during synthesis or post-synthetic) enable a host of strategies to both improve crystalline order for more stable and higher surface, as well as add metals with open coordination for enhanced H₂ binding enthalpy.

Key Accomplishments:

- All milestones up to Go/No-Go milestone were met (see Milestone table)
- Achieved 15-17 kJ/mol activation energy for H₂ desorption for metallated COF
- Achieved high surface area (1700 m²/g) for COF through improved crystallinity
- Achieved sample density equal to crystalline density through COF compaction with < 10% loss of surface area
- Synthesized and characterized roughly one dozen novel COF materials
- The manuscript “Phenyl/Perfluorophenyl Stacking Interactions Enhance Structural Order in Two-Dimensional Covalent Organic Frameworks” was published in *Crystal Growth and Design*.
- The manuscript “Thermal Activation of a Copper-Loaded Covalent Organic Framework for Near-Ambient Temperature Hydrogen Storage and Delivery” was published in *ACS Materials Letters*.
- One manuscript is in progress on COF densification and set to be submitted this FY
- Developed and benchmarked various techniques specifically for COF/metallated COF characterization at NREL through HyMARC, including TPD, DRIFTS, XRD, PCT, and TEM
- Initiated collaborations with Mike Toney (SSRL), Keith Ray (LLNL), and Jeff Long (LBNL) for characterization and modelling of COF materials
- Presented results at ACS, MRS and DOE meetings
- Funded research at Colorado School of Mines for graduate students toward Master’s and PhD degrees

Executive Summary:

Overall, we made significant progress toward synthesizing, upscaling/optimizing, and characterizing about a dozen covalent organic frameworks for structural and gas sorption properties. We found the long-range order (i.e. crystallinity and porosity) is greatly improved through rational fluorine substitution, which is a key element toward raising the ceiling on hydrogen storage capacity for COFs. The H₂ sorption characteristics of the COFs also vary with fluorine substitution but not in a predicted fashion. Despite calculations that predict > 8 kJ/mol binding energies, the fluorinated COFs show anomalously low H₂ adsorption at 77 K and 1 bar with the current post-synthetic processing procedures. Extensive testing of the FASt-COF with PCT and TPD under various degassing conditions has shown only weak binding and gravimetric capacity of 0.3 wt.% at room temperature and 100 bar. The capacity at 77 K is more reasonable for the high surface area (2.8 wt.%, 1700 m²/g). The non-metallated COFs Base-COF and FASt-COF showed isosteric heat values of approximately 4.5 kJ/mol and 5.0 kJ/mol, respectively. However, it is possible that higher binding enthalpy sites do exist in each COF and are populated with H₂ at low pressures. The values of binding enthalpy appear to trend above 7 kJ/mol, but this was not pursued further. Due to our ability to compress FASt-COF to near the crystalline density without loss of surface area, real volumetric capacities are quite high (roughly 30 g H₂/L).

The metallated COF series are quite interesting both in the influence of fluorine on metal uptake as well as their H₂ sorption properties. Using temperature-programmed desorption (TPD) ramping, we found that a Cu(II) species intercalated into COFs binds H₂ with a desorption activation energy (related to isosteric heat) of about 9-10 kJ/mol. In addition, fluorine appears to broaden the curve and shift it to higher temperatures, consistent with the modulation of Cu(II) Lewis acidity. Conversion to Cu(I) has been confirmed in OH-COF using TPD and TGA, and a distinct H₂ desorption peak in TPD is found near 100°C, which is an indication of very strong physisorption due hydrogen interaction with the metal. X-ray absorption studies have proven both the oxidation state of copper as well as its binding environment. DRIFTS has further confirmed the strong binding of H₂ at the Cu(I) site. TPD at a variable ramp rate showed that the activation energy for H₂ desorption (a proxy for the binding enthalpy) is roughly 15-17 kJ/mol, a nearly ideal value for practical H₂ storage. The gravimetric capacity of the metallated COFs is quite low, and attempts to extract an isosteric heat failed with the time available.

Fluorinated COF materials development summary:

The size and symmetry of the COF precursors determines the pore size and geometry. We chose precursors with trigonal (P3) geometries, resulting in COFs with hexagonal pores with roughly 2.4 nm diameters. These COFs form two-dimensional sheets in analogy to graphene that stack to form three-dimensional crystallites. The strength of van der Waals binding between stacks determines the degree of crystallinity, which is limited by defects and disorder resulting from geometrical distortions. Strengthening interlayer interactions and improving planarity are strategies for enhancing the long-range order in the stacking direction. We built the following COFs in the first stage of the project: (i) Base-COF (also referred to as COF-1) with no additional functionalization; (ii) OH-COF (also referred to as COF-2) with a hydroxyl group adjacent to the imide nitrogen, which can subsequently undergo hydrogen bonding which planarize the chains; (iii) FASt-COF (also referred to as COF-3), which is partially fluorinated and can undergo a unique stacking pattern in which consecutive layers are rotated by 60 degrees to produce an alternating phenyl/perfluorophenyl pattern; (iv) a nearly fully fluorinated COF with fluorines in all possible positions except for the phenyl groups at the COF nodes (also referred to as COF-4); (v) FOH-COF, which includes features of both FASt-COF and OH-COF. COFs (i)-(iv) are depicted below with their precursors.

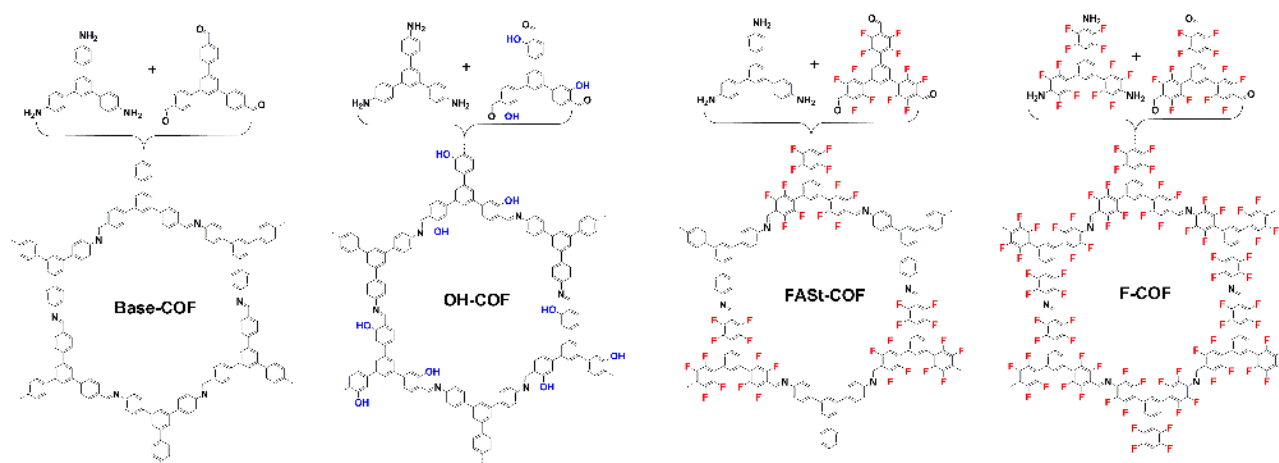


Chart 1. Precursors and structures for COFs associated with Milestones 1.1 and 1.2.

Synthesis of COFs

Precursors for the Base-COF and OH-COF were reacted at 120 °C for 3 days in a mixture of 1.9/0.1/0.1 parts *o*-dichlorobenzene, 1-butanol, and 6M acetic acid. The COF materials precipitate after several minutes at the reaction temperature, but countless studies have demonstrated that the surface areas of COF materials continue to improve if left to react for ~3 or more days under these conditions. The moisture and alcohol in the reaction mixture are essential to achieving higher degrees of crystallinity and larger surface areas as they promote a certain degree of reversibility in the condensation reaction that allows for defects in the COF structure to be “repaired” with time. These COFs were recovered in >95% yield.

After synthesis of the fluorinated tris-amine in Chart 1 in one step from a literature procedure, the compound was reacted with the non-fluorinated tris-aldehyde in an attempt to synthesize an alternating stacking COF. However, the highly fluorinated tris-amine is a very poor nucleophile and no reaction was observed with the tris-aldehyde over the course of 1 week at 120 °C, even when

moisture and alcohol were removed to push the reaction towards the product as much as possible. However, by fluorinating the tris-aldehyde component instead, a highly reactive electrophile was generated that was very reactive with a non-fluorinated amine. The reaction proceeded so quickly that FAST-COF product began precipitating as soon as the monomer components could dissolve and before the acetic acid catalyst was injected. The final product was recovered in ~98% yield. The highly fluorinated F-COF was produced from the strongly reactive fluorinated tris-aldehyde and the weakly reactive fluorinated tris-amine, though the reaction was quite slow; F-COF precipitate was not observed during the first several hours of the reaction, and the final material was only recovered in ~40% yield.

Structural characterization of non-metallated COFs

The surface areas of the four materials were determined through nitrogen sorption measurements at 77K (Figure 1 and Table 1). The BET surface area of the Base-COF was measured as $970 \text{ m}^2\text{g}^{-1}$ using our optimized conditions, which is more than double the literature optimized value,¹ though less than 50% of its theoretical Connolly surface area.

The introduction of hydrogen bonding groups in the OH-COF improves the BET value to $1410 \text{ m}^2\text{g}^{-1}$, though this is still only about 75% of its theoretical Connolly value. We note that the Connolly values for the F-COF and FAST-COF decrease from the Base-COF, due to added mass and pore filling, but the BET surface areas improve to $1275 \text{ m}^2\text{g}^{-1}$ for the F-COF and $1700 \text{ m}^2\text{g}^{-1}$ for the FAST-COF, the latter fulfilling the theoretical value to within uncertainty. The improvement is likely a function of the intrinsic material design that maximizes alternating phenyl/perfluorophenyl stacking interactions. This and the subsequent characterization are the subject of a published paper.¹

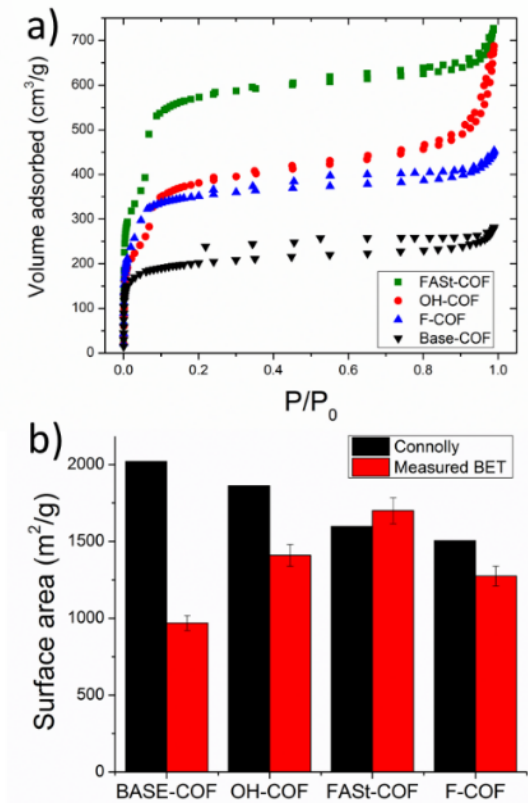


Figure 1. (a) BET isotherms for each COF. (b) Measured BET values vs. Connolly areas.

Table 1. Structural parameters of COFs.

	Base-COF	OH-COF	FASt-COF	F-COF
BET (m ² /g)	970	1410	1700	1275
Connolly area (m ² /g)	2020	1862	1598	1505
Pore volume (cm ³ /g)	0.40	0.69	1.09	1.00
Stacking distance (Å)	3.64	3.64	3.58	3.79
Density (g/cm ³)	0.55	0.58	0.70	0.83

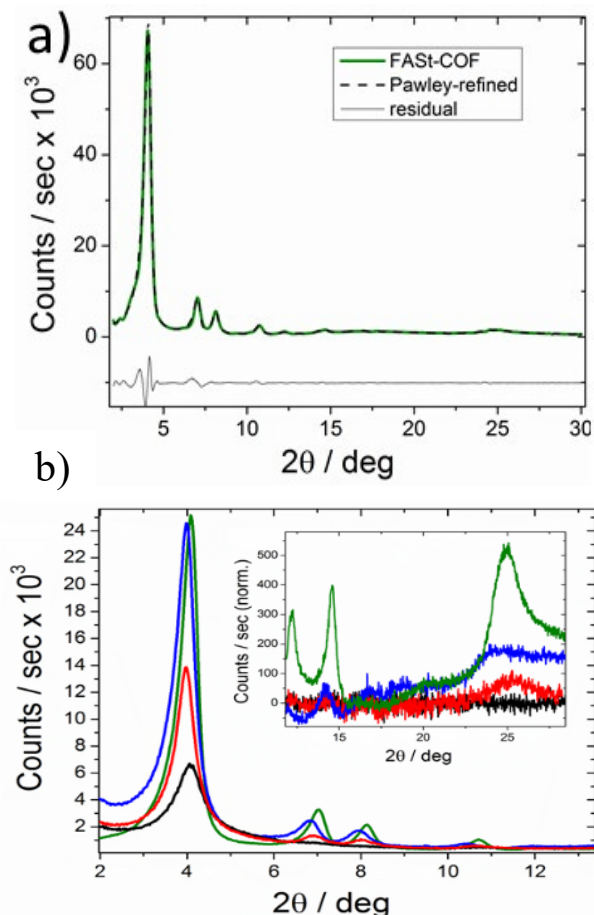


Figure 2. a) Pawley-refined XRD pattern for FAST-COF. (b) Peaks at lower and higher (inset) angles for each COF.

X-ray diffraction (XRD) of the COF powders, Figure 2, demonstrates a remarkable increase in long-range order through the sample series. All COFs show a prominent (100) peak at about 4°, and the expected series of peaks at higher angles previously observed for a similar COF family.² For the Base-COF these peaks are broad and become indistinguishable from noise after the (110) peak. Much narrower (210) and higher peaks are found for the OH-COF, F-COF and FAST-COF. However, OH-COF peaks above 10° are broad and difficult to distinguish from the background. The (001) peak that reflects the COF interlayer spacing (parallel to the crystal c-axis), is narrowest for FAST-COF and is found at about 25°, significantly shifted from the broad (001) peak found for F-COF at 24°. The shift combined with the decreased width is evidence for tighter interlayer stacking that results from strong interactions for the FAST-COF.

The COFs remain stable to high temperatures, as evidenced by their thermogravimetric analysis profiles, Figure 3. Less than 2% mass loss is incurred up to 350°C, with material breakdown between 450-600°C. This high degree of stability is a desirable property both for potential post-synthetic modification reactions that might occur at elevated temperatures, as well as for practicality in a variety of conditions.

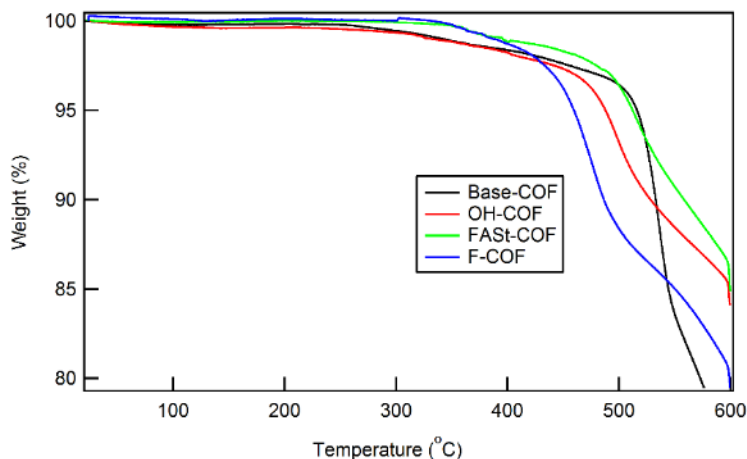


Figure 3. TGA curves for COFs

Diffuse reflectance infrared spectroscopy (DRIFTS) was performed on all COFs. The spectra and their assignments for FAS-COF and Base-COF are shown in Figure 4. The bands associated with C-H, C-C, C-N, and C-F bonds are illustrated. Aliphatic C-H stretch bands were seen in the Base-COF despite none expected from the molecular structure. These are presumably from solvent or other hydrocarbon contamination. The relative proportion of aliphatic bands was higher for FAS-COF, suggesting increased proclivity for hydrocarbon sorption when fluorine is present. We spent time to develop supercritical CO₂ and other solvent extraction techniques to remove these contaminants that may reduce the activity of the material for gas sorption. Clear evidence of C-F stretch bands were seen in the FAS-COF but not in the Base-COF, as expected. H₂ gas at low pressure was introduced into the COF during the DRIFTS measurement at room temperature, and spectra did not show new bands that would be associated with a chemical reaction with the COF. Experiments at UC-Berkeley did not show a clear H₂ peak, probably due to low capacity and weak binding.

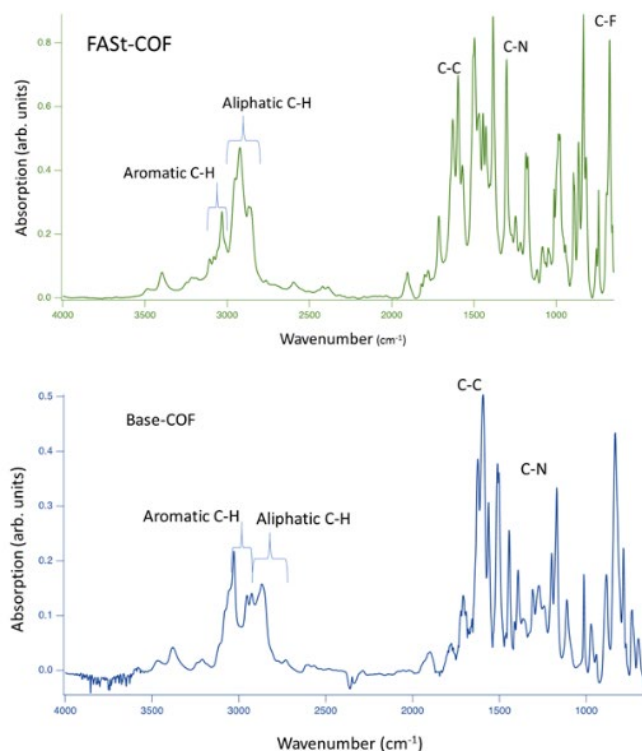


Figure 4. DRIFTS spectra of FAST-COF and Base-COF powders, showing C-H region and fingerprint region. Note residual alkane peaks near 2800 cm^{-1} .

Further structural characterization of COF series 1

We obtained transmission electron microscopy (TEM) images of the four COFs from Chart 1 in order to evaluate how changes in layer stacking would affect the crystallite habit and size. The images are shown in Figure 1, and they reveal much larger and more well-defined crystallites for FAST-COF better crystallinity on long length scales. The other COFs show smaller crystallites and larger regions that appear to have no clear structure, Figure 5a-c. compared with other COFs. Some rod- or tube-like structures are found to be at least a few microns in length, Figure 5d-e. These features are further indicators that local ordered stacking is leading to longer range ordering.

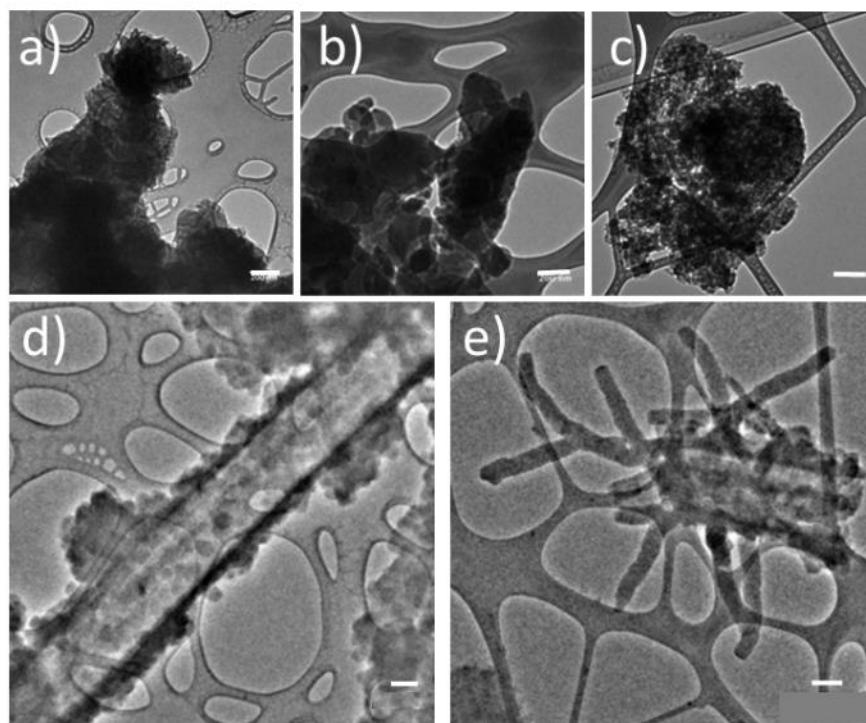


Figure 5. Representative TEM images of a) Base-COF, b), OH-COF, c) F-COF, and d)-e) FAST-COF. Scale bar is 200 nm for all images.

Calculations of the cohesive energy of the alternating stacked crystal of FAST-COF, Figure 6a, result in a stabilized crystal structure compared with the directly stacked version, Figure 2b. The cohesive energy is 28 kJ/mol higher per six phenyl groups for the alternating structure. This confirms that the COF design allowing for alternating stacking is successful.

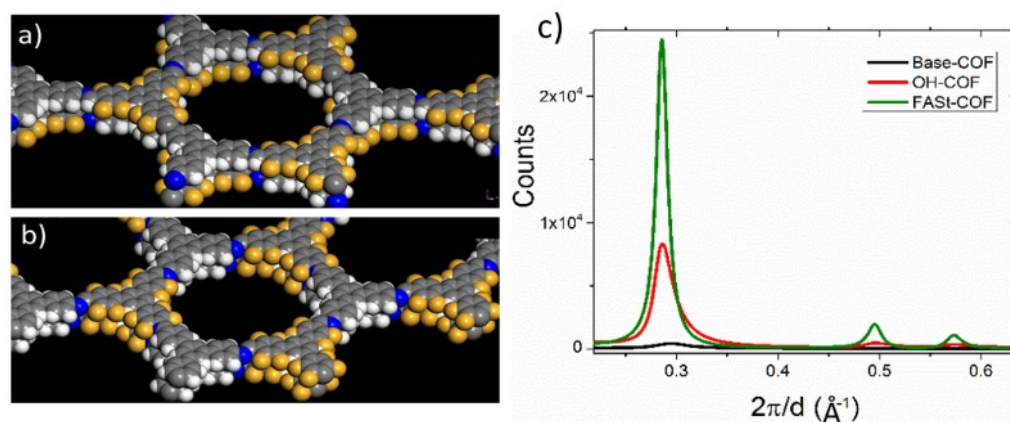


Figure 6. FAST-COF (a) alternating and (b) direct stacked structures. (c) SAXS data for three of the COFs.

Small angle X-ray scattering (SAXS) at the Stanford linear accelerator (SLAC) confirmed the results previously obtained with powder XRD at NREL, Figure 6b. All COFs show a prominent peak at a d-spacing of 22 Å, which is the periodicity distance in the plane of the COF. The FAST-COF peaks are much narrower than those of the other COFs. We have a sample cell that can be pressurized up to 100 bar of H₂, which we will use to monitor structural changes with pressure.

Hydrogen Sorption Characteristics

PCT on non-metallated COFs

The results of pressure/composition/temperature (PCT) measurements temperatures are shown in Figure 7. For 149 mg of FAST-COF at 76K, the isotherm rises sharply and plateaus around 40 bar at an excess gravimetric capacity of about 2.8 wt. %. At higher temperatures, the isotherm shape is shallower, and the maximum uptake value shifts to higher pressure. At 303 K and 100 bar, the excess gravimetric capacity value is about 0.3 wt. %.

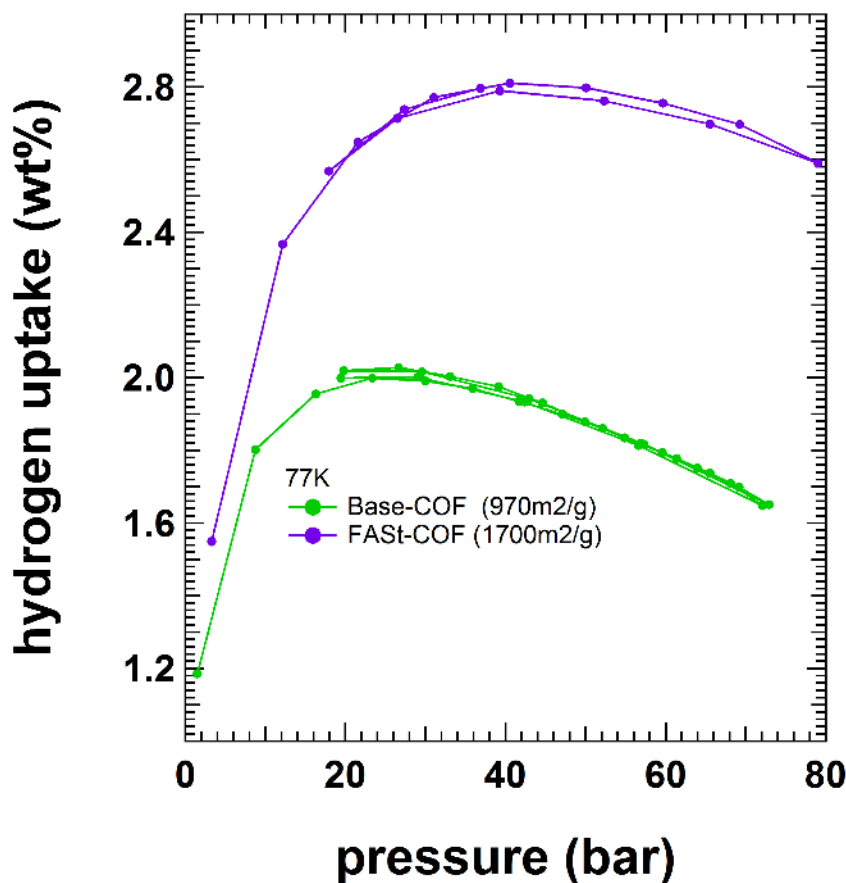


Figure 7. Excess capacity plots from PCT analysis of Base-COF and FAST-COF at 77K.

The results of extensive pressure/composition/temperature (PCT) measurements with > 500 mg of material are shown in Figure 8, following the van't Hoff analysis using the curves at 77K and 87 K. In each case > 0.5g of material was used. The reason that the lower temperature isotherms are used is that the capacity adsorbed at higher temperature is very small, which can lead to significant errors when determining Q_{st} . The relatively flat region from about 2-5 moles can be used for Q_{st} determination. This can be considered the average value of binding for multilayer H₂, and is higher for FAST-COF than Base-COF by 0.5-1 kJ/mol. This increase was previously predicted by DFT calculations from LLNL. The upturn at low adsorption may be an indication of higher binding enthalpy sites, in particular near the imide nitrogens. These sites were also used in the calculations and led to binding enthalpy values around 8-9 kJ/mol. DRIFTS measurements at Berkeley were performed on these COFs to determine the binding enthalpy at low temperature and under micro-dosing conditions but did not provide conclusive values.

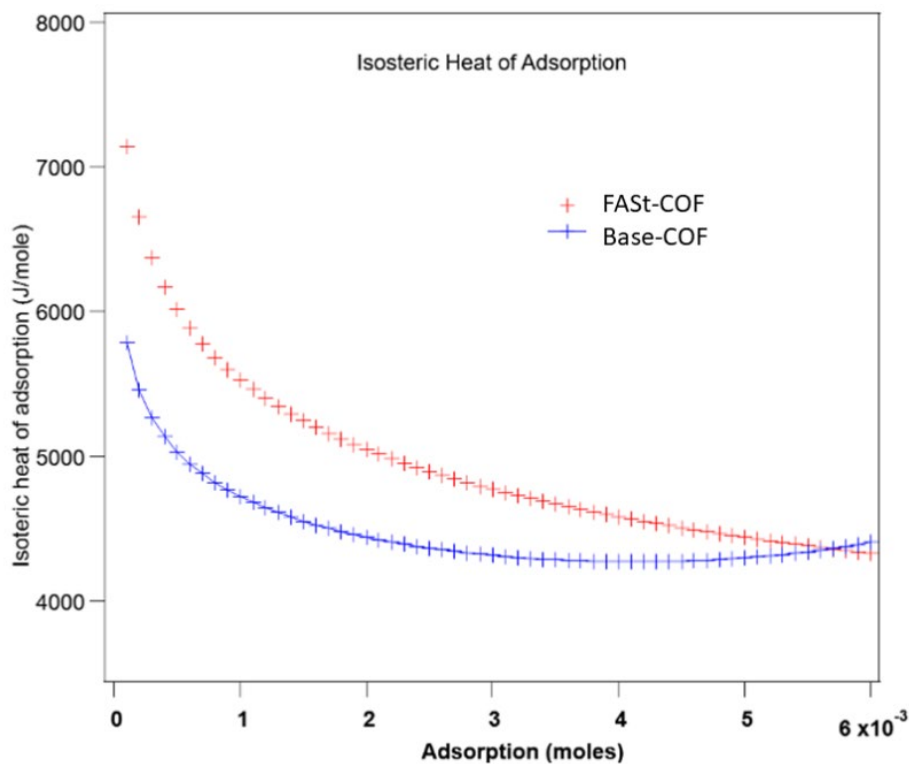


Figure 8. Isosteric heat plots for Base-COF and FAST-COF using PCT curves at 77K and 87K.

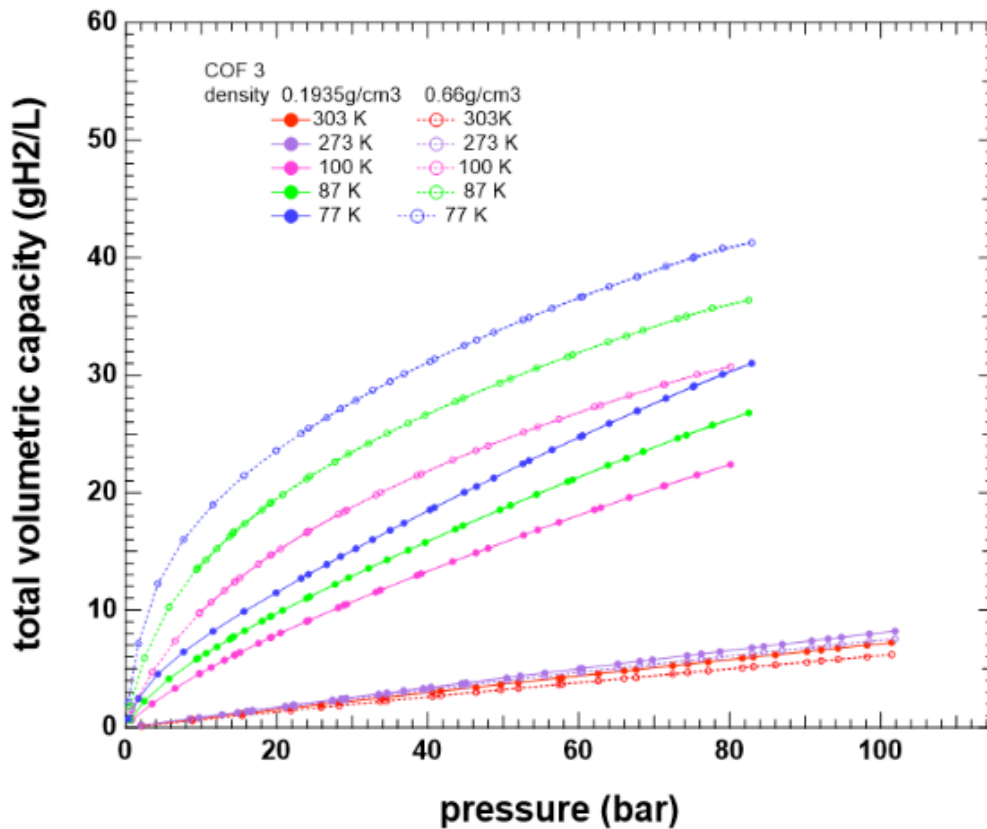


Figure 9. Total volumetric capacity from PCT for FAST-COF at different temperatures and including measured powder density (closed circles) and crystal densities (open circles).

The total volumetric capacity for FASt-COF, Figure 9, was calculated using excess gravimetric capacity and the details of sample density and volume from PCT measurements. Although PCT measurements were terminated at about 80 bar pressure, we can extrapolate the results to 100 bar to arrive at a value of about 30 g/L at 77K for the densified samples. We found that FASt COF in particular is amenable to significant densification (>90% of crystal value) without loss of surface area (discussed below).

With the roughly 3 wt. % gravimetric capacity for a BET surface area of 1500 m²/g, FASt-COF falls slightly short of achieving the milestone of 4 wt. %. However, we have previously achieved 1700 m²/g with FASt-COF (corresponding to roughly 3.5 wt. %), and we believe that employing improved crystallization techniques¹ would allow us to approach 2000 m²/g, especially if the amount of fluorine is reduced. Not enough time/resources existed to pursue these synthetic routes.

Calculations

We initiated teleconferences and data/information sharing with Brandon Wood and Keith Ray in the HyMARC consortium for computational support and prediction of structure and H₂ binding characteristics of the COFs we have synthesized and plan to synthesize. Theoretical work at LLNL has focused on the determination of the change in H₂ binding energy at two binding sites across a series of five COFs that differ in the chemical functionalization of the carbon rings. Due to the weak interlayer forces, the computational geometry optimization of these materials takes a large number of relaxation iterations.

The change in H₂ binding energy at two binding sites across the series of four COFs was determined, Figure 10. The binding energy of hydrogen to the Base-COF is roughly 8-9 kJ/mol, which is the lowest among the series, regardless of the binding site. H₂ binding energies for the other COFs range from 9-11 kJ/mol, depending upon the binding site. These results lend some support to the notion that fluorination should enhance binding enthalpy above 10 kJ/mol, which is one of the targets in our Go/No-Go milestone. Binding geometries metals in the new series of metal-binding COFs (see Figure 11) were also calculated, initially using Cu(II) chloride as the intercalant. Subsequently, H₂ binding enthalpies in close proximity to those metals have been estimated at 10-25 kJ/mol. Further exploration was cut short by the project termination.

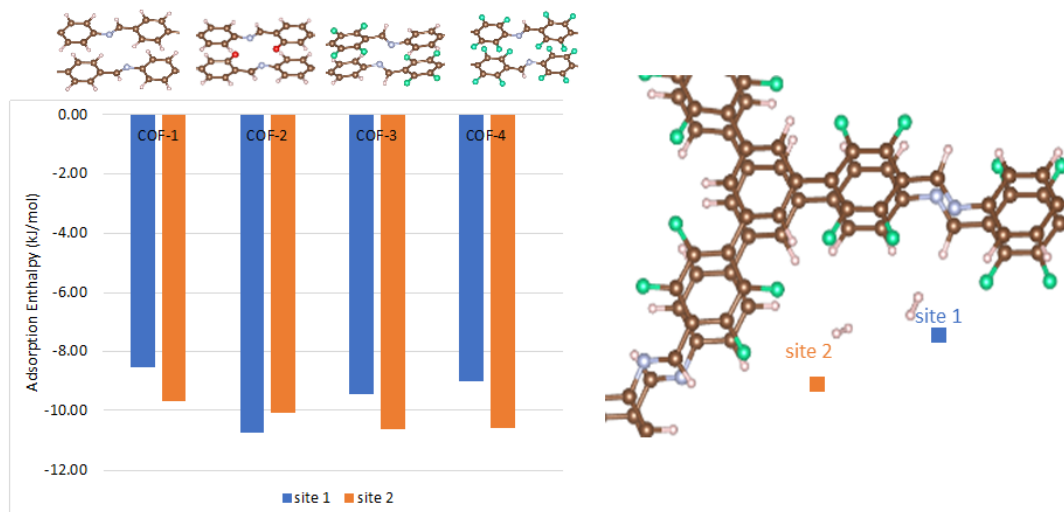


Figure 10: Relaxed structures and sites for H₂ binding. Calculated adsorption enthalpies for non-metallated COFs.

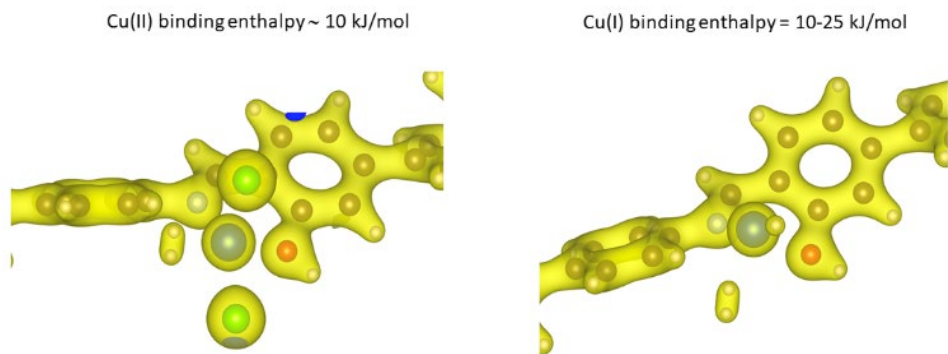


Figure 11. Binding geometries for Cu(II) and Cu(I) that give rise to varying binding enthalpies.

COF Densification

The volumetric capacity of a sample for gas storage is closely related to its density, and thus compacting the normally void-filled COF powders has advantages. The COF-3 (FASt-COF) and COF-1 (Base-COF) materials were densified using a pellet press capable of variable pressures with a known pellet area. The thickness was measured, and with the known mass, a density was calculated for a variety of pellets, Figure 12. The COF-3 pellets were made up to and above the predicted crystalline density, and it was found that the N_2 BET surface area was almost constant vs. pellet density. Small angle x-ray scattering (SAXS) confirmed that very little structural change was occurring upon compression. This contrasts with COF-1 compression, which shows both a lower BET SSA and broader XRD peaks with increasing pellet density (data not shown). We attribute this change to the ability of the partially fluorinated COF-3 to undergo structural rearrangements to reduce void space while maintaining strong stacking interactions facilitated by the perfluorophenyl-phenyl interactions. This strategy could be used to densify COF or MOF powders into pellets that can achieve larger volumetric capacities for H_2 storage.

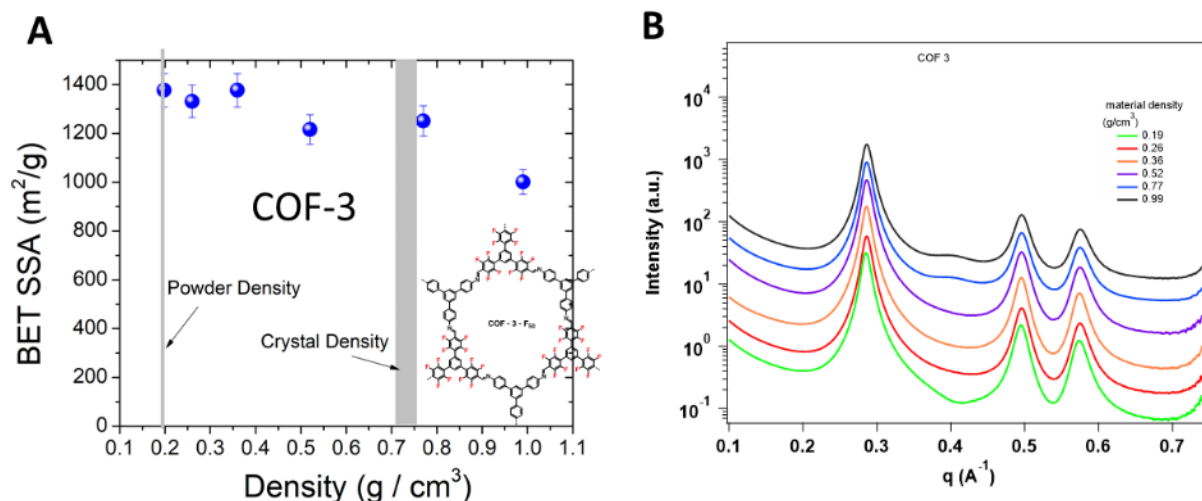


Figure 12. (A) BET surface area vs. measured density of sample. Predicted crystal density is shown as gray bar. (B) SAXS data showing negligible change in structure vs. density.

COFs for metalation

Milestone 1.2 involves the synthesis of COFs with specific binding sites for metals, and fluorination at strategic positions. The COFs in Chart 2 were synthesized in small amounts for initial testing. Scale-up was then pursued, and the material has been partitioned into several fractions for attempting the metalation strategies. The binding sites are N-N imide-aniline sites (with and without proximal fluorines), and OH-N phenol-imide sites. The OH-N COF without fluorines is the same as the previous OH-COF, which we have studied in detail. Preliminary characterization using BET and XRD suggest slightly lower crystallinity and surface areas for these new COFs compared with FAST-COF but still in a reasonable range (1000-1500 m²/g). We have gone forward with intercalation studies with copper (II) species, finding clear evidence of Cu binding. Some loss of crystallinity was also observed after metalation, detected by powder XRD. NEXAFS studies at SLAC have been performed on the metalated COFs, and results show clear evidence of Cu-N binding. Other metalation strategies and other metals were meant to be attempted, but time and resources for synthesis or guidance from theory were not available.

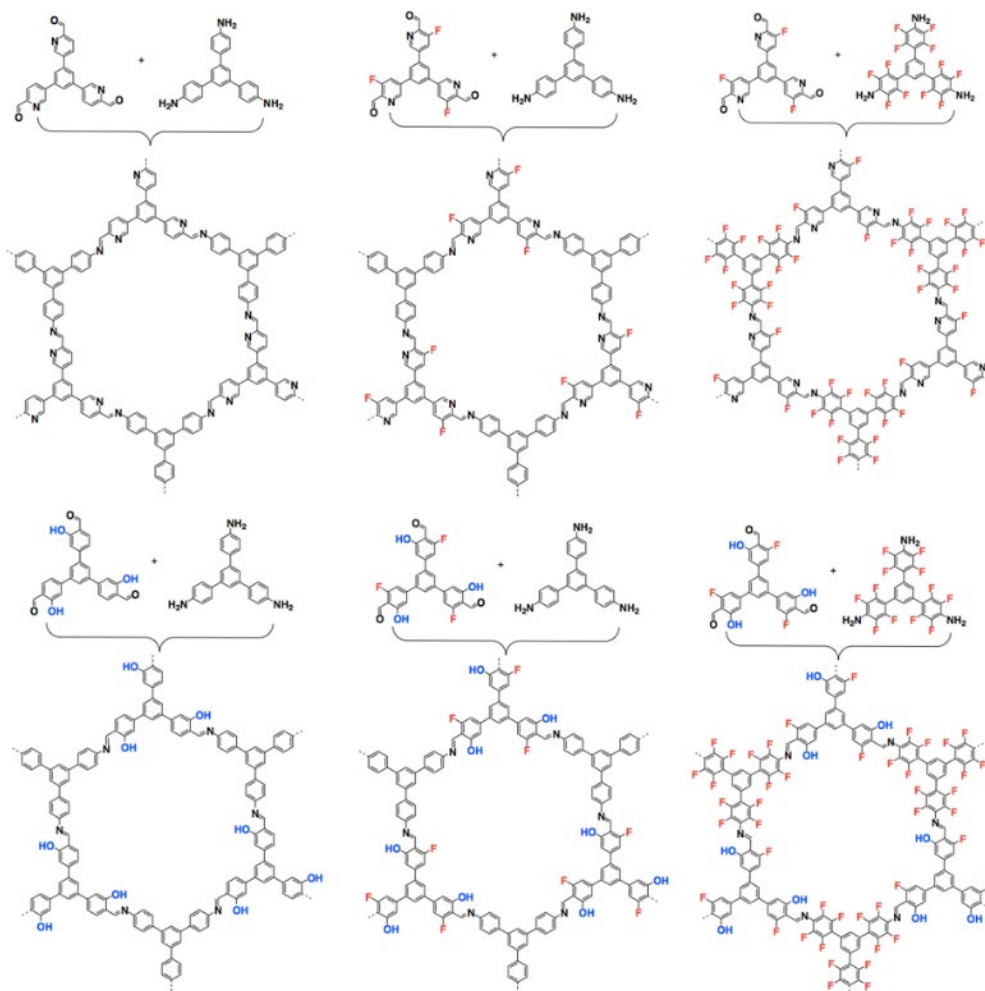


Chart 2. Synthesized COF structures with metal binding sites.

The COFs in Chart 2 were eventually synthesized in roughly 100 mg amounts for preliminary measurements of BET, TPD, DRIFTS, and X-ray spectroscopy. We performed intercalation studies with two types of copper (II) species into the COFs with imide-aniline sites (the two in the upper left of Chart 2) and with all COFs on the lower row with hydroxyl-imide sites. Copper intercalation has been most successful in the COFs with no fluorines, which we believe is due to the electron-withdrawing character of fluorine that reduces the nucleophilic nature of the O and N binding sites. Thus, the equilibrium between solvated metal and COF-bound metal skews toward solvated metal when the COFs are soaked in copper salt solution. This is an unintended consequence of fluorination, but there are potentially ways to circumvent this problem. Choosing a different solvent system or using vapor-phase metal intercalation are methods we are exploring. For the OH-COF, we used electron dispersive spectroscopy (EDS) in an electron microscope to determine that copper constitutes about 13 wt% of the total COF. If we estimate the COF ring molecular weight as approximately 2300 grams (as shown in chart 2, lower left), then 13 wt% copper constitutes about 5 copper atoms. There are six sites per ring, thus the COF is nearly fully loaded with copper. ICP elemental analysis was also performed and found to largely agree with the EDS results.

Electronic Structure of Metallated COFs

X-ray absorption spectroscopy is a powerful technique for probing local structures without any requirements for long-range order in the material. Furthermore, the oxidation state of a metal can be obtained from the X-ray absorption near-edge structure (XANES), while information regarding that metal's coordination sphere can be extracted from the extended X-ray absorption fine structure (EXAFS).³ As shown in the blue XANES spectrum at the top of Figure 13 corresponding to the Cu(II)-COF, a pre-edge energy of 8977.6 eV is observed in a range typical of Cu(II) species.³ The formation of Cu(I) following the thermal treatment that evolves CO₂ is confirmed by XANES with the disappearance of that pre-edge energy and the appearance of the edge energy at 8981.8 eV, which is fully consistent with edge energies associated with Cu(I) in the literature.³⁻⁵ Furthermore, the overall decrease in intensity of the spectrum associated with the oxidation state change would be consistent with a decrease in overall Cu coordination.

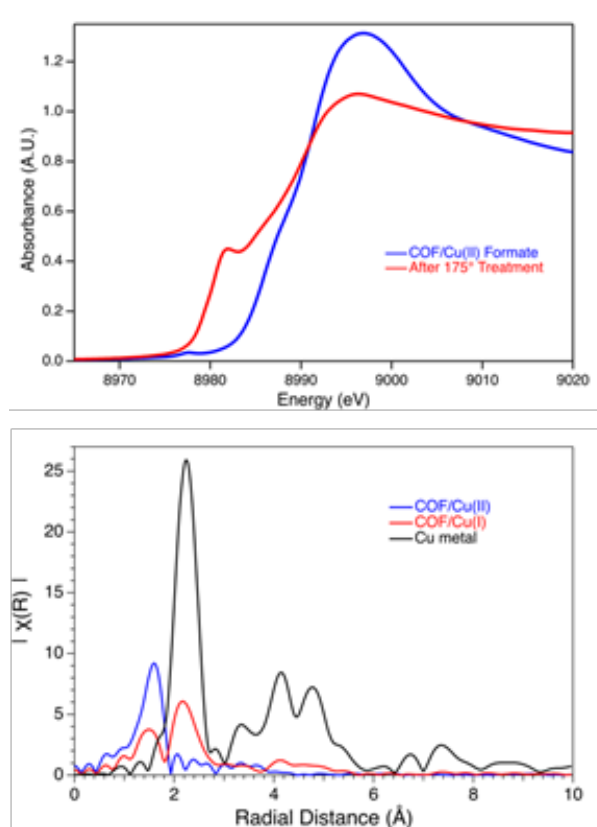


Figure 13. (Top) X-ray absorption near-edge structure (XANES) of Cu-loaded COF, before and after thermal treatment, demonstrating definitively the reduction to the Cu(I) oxidation state. (Bottom) Extended X-ray absorption fine structure (EXAFS) of the Cu-loaded COF in its two oxidation states plotted alongside that of Cu(0) metal.

The decrease in the feature at ~ 1.5 Å in the EXAFS spectrum (Figure 13, bottom) following thermal treatment of the Cu-COF (compare red and blue traces) is also consistent with a reduction in the coordination sphere of Cu that would be associated with the loss of the formate anion and Cu-O bonds. Interestingly, a new feature at ~ 2.2 Å develops following thermal treatment of the Cu-COF. This feature is consistent with the major feature observed in a Cu(0) metal sample (black trace) and would thus be consistent with the formation of some new Cu-Cu interaction, plausibly the result of coordinatively unsaturated Cu(I) species being in close proximity above and below each other in different 2D COF “planes”.

Hydrogen sorption for metallated COFs

The metallated COF series are quite interesting both in the influence of fluorine on metal uptake as well as their H₂ sorption properties. Using temperature-programmed desorption (TPD) ramping, we found that a Cu(II) species intercalated into COFs binds H₂ with a desorption activation energy (related to isosteric heat) of about 9-10 kJ/mol. In addition, fluorine appears to broaden the curve and shift it to higher temperatures, consistent with the modulation of Cu(II) Lewis acidity. Conversion to Cu(I) has been confirmed in OH-COF using TPD and TGA, and a distinct H₂ desorption peak in TPD is found near 100°C, which could be an indication of very strong physisorption (> 20 kJ/mol), or copper hydride formation.

Copper (II) chloride was intercalated into COF-6 and COF-7, and TPD studies were performed with H₂, Figure 14. The partially fluorinated COF-7 shows the highest and broadest H₂ desorption peak. These results would suggest that Cu is enhancing the binding enthalpy through the effect of the fluorines proximal to the Cu.

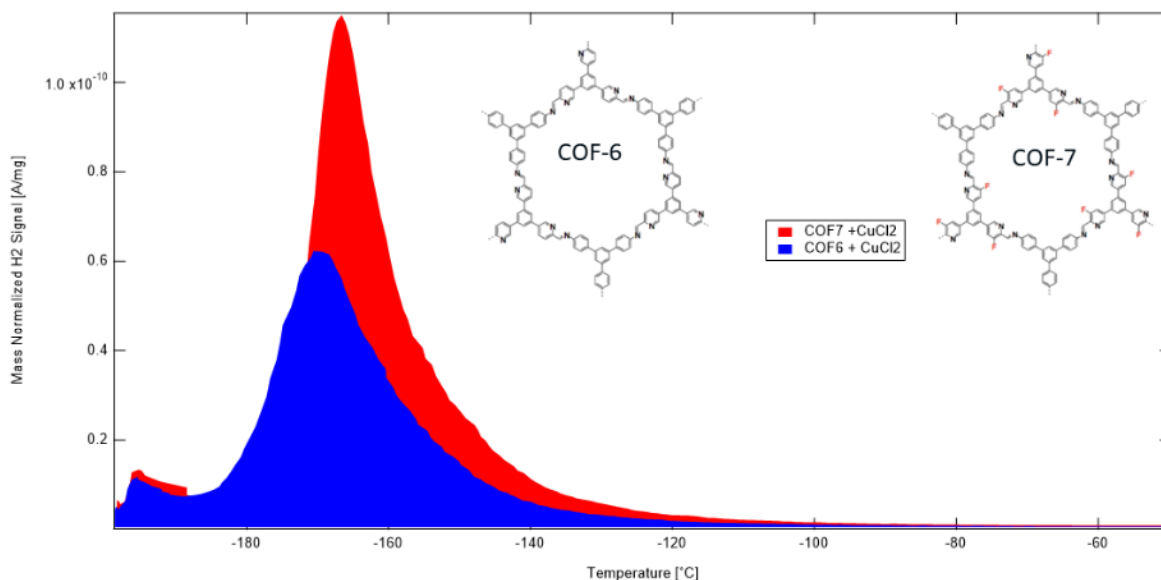


Figure 14. Temperature-programmed desorption (TPD) of COF-6 and COF-7 intercalated with CuCl₂. Obtained by Madison Martinez (NREL), HyMARC.

To determine a rough estimate of H₂ binding enthalpy, a temperature ramping study was done with Cu(II) intercalated into COF-1. We found that the activation energy for desorption is roughly 9-10 kJ/mol., which is expected based on results from MOFs.⁶ Based on the results in Figure 3, we anticipated that the activation energy should be even higher for COF-3 due to the influence of fluorination; however, due to the large degree of fluorination we found that COF-3 did not uptake significant amounts of Cu. To determine the enhancement of H₂ binding enthalpy in fluorinated systems may require a different approach to metallation. We have begun using vapor-phase intercalation using a Cu(I) precursor that has been previously used for atomic layer deposition. This precursor was introduced into COF-1 and COF-3 powders, and the expectation is that Cu will bind to the COF pores. Because the Cu(I) precursor ligands are thermally labile, we predict that we can heat the COF under vacuum to uncover Cu sites for binding. ICP analysis and TPD will be used on these COFs to determine the viability of vapor phase metalation.

Converting Cu(II) centers to Cu(I) species can be accomplished in-situ after Cu binding to COF sites. We performed a thermal treatment after copper (II) formate intercalation into COF-2 (OH-COF). We discovered that upon heating to 160C, a mass loss was observed in TGA, and a large peak at m/z=44 for CO₂ was detected, Figure 15. These observations are consistent with the reduction of Cu(II) to Cu(I) and the subsequent release of CO₂ gas (and probably also the production of formic acid, which is more difficult to detect). This conversion is reproducible and occurs at higher temperatures for COF-9 and COF-10, the fluorinated analogs of COF-2, which would be expected to possess more strongly bound formate ligands due to the enhanced Lewis acidity of the Cu.

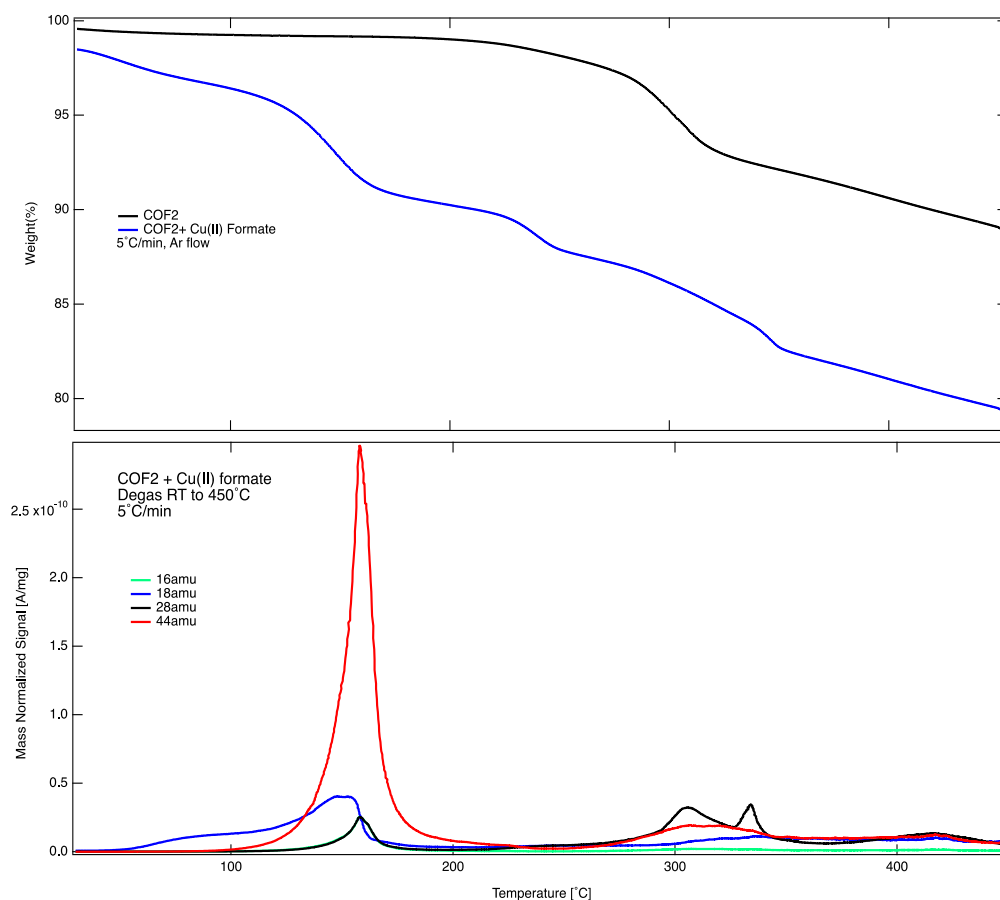


Figure 15. Top, thermogravimetric analysis (TGA) of COF-2 before (black) and after (blue) metalation. Bottom, temperature-dependent desorption signal for COF-2 intercalated with Cu(II) formate. Red peak is CO₂.

Interestingly, the TPD results before and after thermal reduction of Cu in COF-2 are strikingly different, Figure 16. Although a low temperature desorption peak at about -140C representative of physisorbed H₂ remains similar in both samples, a peak near 100C is found for the Cu(I) COF. We are currently exploring the conditions that produce this peak, but it may be related to a Cu(I) hydride species or a strongly physisorbed species. We intended to use fluorination, such as in COF-9 and COF-10, and other linker modifications to adjust the H₂ desorption temperature. We also intended to explore methods for increasing the amplitude of this peak through improved copper intercalation methods (e.g., linkers with additional binding sites, vapor phase deposition). These strategies could be the subject of future work.

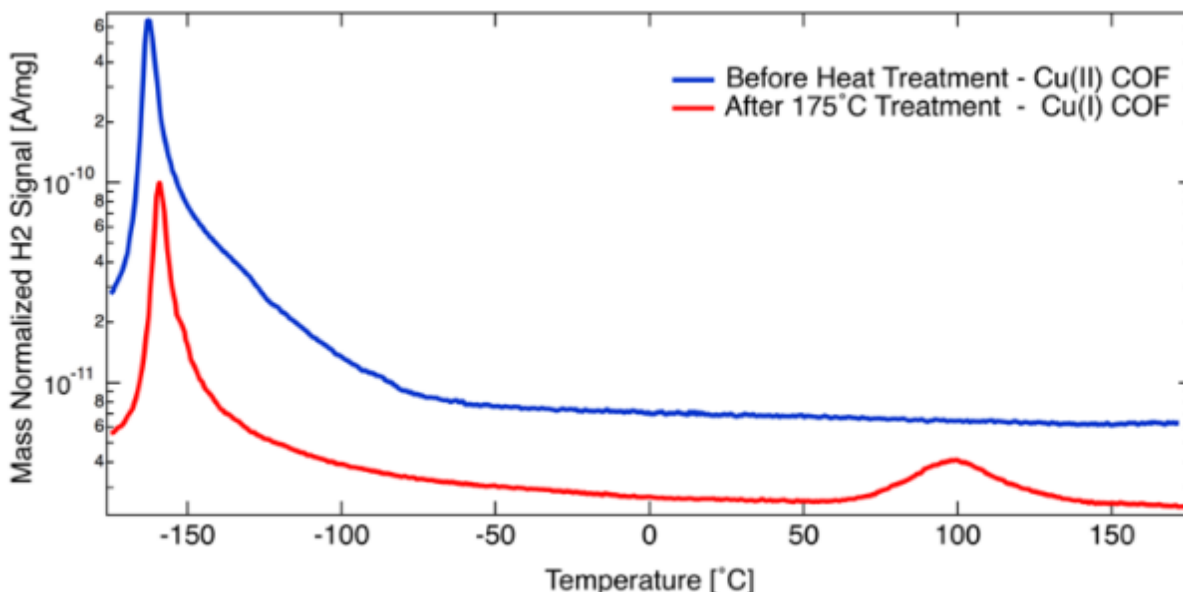


Figure 16. H₂ TPD results for Cu formate intercalated into COF-2 (OH-COF). Red curve is for Cu(I), which shows a peak near 100C. Blue curve is for Cu(II).

H₂ desorption from the thermally activated Cu(I)-COF is plotted as a function of ten different heating rates (β) in Figure 17. For these ramp rates, the peak temperature (T_M) for H₂ desorption varies between r.t. and nearly 150 °C. Analysis of the data according to the well-established Kissinger method, a universal approach for analyzing thermally activated transformations,⁷ allows us to estimate the activation energy of H₂ desorption from a linear fit of a plot of $\ln(\beta/T_M^2)$ vs. $1/T_M$ (not shown). The data suggests the activation energy for H₂ desorption from this Cu(I)-COF to be near 17 kJ mol⁻¹, which is considered optimal for ambient temperature H₂ storage and delivery.

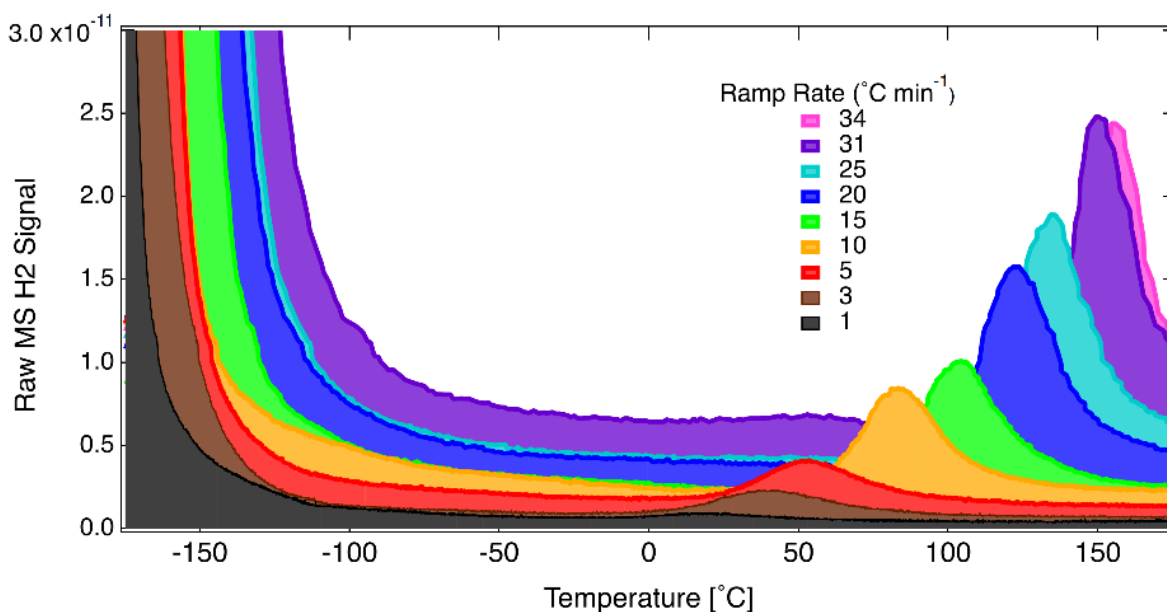


Figure 17. Variable temperature ramp rate data illustrating H₂ desorption for Kissinger analysis.

Final Materials Performance Table

	COF-2 plus Cu Expt (PCT batch)	Theoretical	COF-3 (no metal) Expt (PCT batch)	Theoretical
BET SA (m ² /g)	1000 (1410 ^a)	~2000	1500 (1700 ^a)	1900
Excess H ₂ Wt % (77 K)	2.1	4.2	2.8	4.0
Total g H ₂ /L (77 K, 100 bar)	30 ^c	43	30 ^b	45
Binding energy (kJ/mol)	17 ^e	10-25	--	8-9 ^d
Q _{st} (kJ/mol)	7.2 (273K/303K)		5.0 (77K/87K)	

^a separate batch

^b using achieved pellet density with <10% SSA loss

^c using predicted crystal density

^d DFT calculations

^e activation energy from temperature ramp TPD

Milestone Table

	Milestone Number*	Milestone Description (Go/No-Go Decision Criteria)	Milestone Verification Process	Anticipated Date/Month	Status
Milestone	M1.1	produce 100 mg of pure COF-0, COF-OH, COF-F50, and COF-F100	Elemental analysis (NREL/CSM)	2	100%
Milestone	M2.1	determine relative degrees of enhanced long-range ordering between H-bonding and fluorination strategies	XRD, BET (NREL)	3	100%
Milestone	M3.1	determine influence of strategic fluorination on H ₂ adsorption enthalpy through solvent and modified linker adaptations	FTIR, NMR, TPD, PCT (NREL)	9	100%*
Milestone	M1.2	Synthesize 100 mg of COF series (1 and 2) with linker sites for metal chelation	Elemental analysis (NREL/CSM)	8	100%
Milestone	M2.2	Metallate COFs and determine influence of fluorine on enhanced binding of H ₂ at metal sites	XPS, DFT, TPD (NREL)	11	100%
Go/No-Go	GN1	Produce a COF with at least 4% excess gravimetric capacity and at least 40 g H ₂ /L total volumetric capacity at 77K and 100 bar. COF will have isosteric heat of adsorption ≥ 10 kJ/mol for a non-metallated COF or ≥ 12 kJ/mol for a COF with intercalated metals	DOE validation center (NREL)	14	--

References

1. Braunecker et al. *Crystal Growth and Design.*, **2018**, *18*, 4160.
2. Alahakoon, S. B.; McCandless, G. T.; Karunathilake, A. A.; Thompson, C. M.; Smaldone, R. A. *Chem. Eur. J.* **2017**, *23*, 4255
3. G. Zhang, H. Yi, G. Zhang, Y. Deng, R. Bai, H. Zhang, J. T. Miller, A. J. Kropf, E. E. Bunel and A. Lei, *J. Am. Chem. Soc.*, **2014**, *136*, 924-926.
4. C. Lamberti, S. Bordiga, F. Bonino, C. Prestipino, G. Berlier, L. Capello, F. D'Acapito, F. X. Llabres i. Xamena and A. Zecchina, *Phys. Chem. Chem. Phys.*, **2003**, *5*, 4502-4509.
5. C. Prestipino, L. Regli, J. G. Vitillo, F. Bonino, A. Damin, C. Lamberti, A. Zecchina, P. L. Solari, K. O. Kongshaug and S. Bordiga, *Chem. Mater.*, **2006**, *18*, 1337-1346.
6. Yan et al. *Acc. Chem. Res.* **2013**, *47*, 296-307.
7. J. Farjas and P. Roura, *Thermochim. Acta*, **2014**, *598*, 51-58.

Next Steps:

Appropriate next steps were largely outlined in detail in the respective sections above. They are listed briefly here:

1. Explore crystallinity strategies for metallated COFs to achieve higher surface areas
2. Investigate nature of H₂ binding to Cu using analytical techniques (DRIFTS, NMR, neutron diffraction)
3. Tune H₂ binding enthalpy to Cu using strategic fluorination
4. Achieve near crystalline density in Cu COFs with densification
5. Measure Capacities for metallated COFs using PCT